Available online at www.sciencedirect.com
SCIENCE DIRECT®
Journal of Pharmaceutical and Biomedical Analysis
33 (2003) 999–1015
JOURNAL OF PHARMACEUTICAL AND BIOMEDICAL ANALYSIS
www.elsevier.com/locate/jpba

Identification of oxidative degradates of the TRIS salt of a 5,6,7,8-tetrahydro-1,8-naphthyridine derivative by LC/MS/MS and NMR spectroscopy—interactions between the active pharmaceutical ingredient and its counterion

Yunhui Wu [a,*], Tsang-Lin Hwang [b], Kimberly Algayer [a], Wei Xu [a], Hong Wang [a], Adam Procopio [a], Laura DeBusi [a], Chia-Yi Yang [a], Bozena Matuszewska [a]

[a] *Department of Pharmaceutical Research and Development, Merck Research Laboratories, P.O. Box 4, West Point, PA 19486, USA*
[b] *Department of Bioprocess and Bioanalytical Research, Merck Research Laboratories, P.O. Box 4, West Point, PA 19486, USA*

Received 20 December 2002; received in revised form 2 June 2003; accepted 1 July 2003

Abstract

The Tris(hydroxymethyl)aminomethane (TRIS) salt of a substituted 5,6,7,8-tetrahydro-1,8-naphthyridine compound (I) in a mannitol-based formulation was stressed at various conditions. Liquid chromatography/mass spectrometry (LC/MS) and liquid chromatography/tandem mass spectrometry (LC/MS/MS) analyses of the stressed samples revealed that oxidation and dimerization were the primary degradation pathways for this compound. ^{1}H- and ^{13}C-nuclear magnetic resonance (NMR) spectroscopy were used to characterize the isolated dimers. The aromatized degradate, N-oxide, amide, and three dimeric products were all confirmed by either LC/MS using authentic standards or NMR spectroscopy. In general, the aromatized product was always the primary degradate produced under all stress conditions. When stressed at 80 °C, the TRIS counterion also underwent thermal degradation to yield formaldehyde in situ which reacted with the parent compound to form a unique methylene-bridged dimeric product and an N-formyl degradate. A minor condensation product between the compound I and the TRIS counterion was also detected in the 80 °C stressed samples. Under 40 °C/75% RH stress conditions, TRIS derived degradates were insignificant, while dimers formed by compound I became predominant. In addition, two hydroxylated products (7-OH and 5-OH) were also detected. Mechanisms for the formation of the oxidative and dimeric degradates were proposed.

Keywords: Tetrahydronaphthyridine; Degradates; Oxidation; Dimerization; TRIS salt; Drug–counterion interaction; LC/MS; Tandem mass spectrometry; NMR

1. Introduction

In the early pharmaceutical formulation development process, different salt forms of acidic and

* Corresponding author. Fax: +1-215-652-5299.
E-mail address: yunhui_wu@merck.com (Y. Wu).

0731-7085/03/$ - see front matter © 2003 Elsevier B.V. All rights reserved.
doi:10.1016/S0731-7085(03)00423-0

basic drug candidates are often evaluated and the lead salt form is selected based on its physical and chemical stabilities, manufacturing processibility, and biopharmaceutics properties [1–3]. To quickly obtain chemical stability of the active pharmaceutical ingredient (API) in the presence of excipients, binary mixtures or simple formulations are usually prepared at this stage to assess the compatibility of the excipients. Accelerated stress conditions such as elevated temperature and humidity are often used to generate potential degradation products in a short period of time. The understanding of degradation pathways plays an important role in the selection of excipients and the formulation manufacturing process.

In this study, the tris(hydroxymethyl)aminomethane (TRIS) salt of compound I (Fig. 1) in a mannitol-based formulation was stressed under various conditions. The selection of the TRIS salt for formulation development was based on the facts that TRIS formed a crystalline and non-hygroscopic salt with compound I and the TRIS salt showed superior stability and processibility. Liquid chromatography/mass spectrometry (LC/MS) and liquid chromatography/tandem mass spectrometry (LC/MS/MS) analyses of the stressed samples revealed oxidation was the primary degradation pathway for the target compound [4]. In addition, reactive oxidative degradates can further react with the parent drug molecules to form dimeric degradates. In general, the aromatized product was always the primary degradate produced under all stress conditions. Under thermal stress conditions (80 °C), the TRIS counterion appeared to be unstable to either react with the parent drug to form adducts or decompose to generate formaldehyde in situ which further reacted with the parent drug to yield unique dimeric degradates. Under 40 °C/75% RH stress conditions, TRIS derived degradates were insignificant while dimers formed by compound I became predominant. In addition, several hydroxylated products were also detected.

2. Experimental

2.1. Chemicals and reagents

Compound I and the synthetic standards of degradates III, IV and X were obtained from Merck Research Laboratories (West Point, PA, USA). HPLC-grade acetonitrile and water were purchased from EM Science (Gibbstown, NJ,

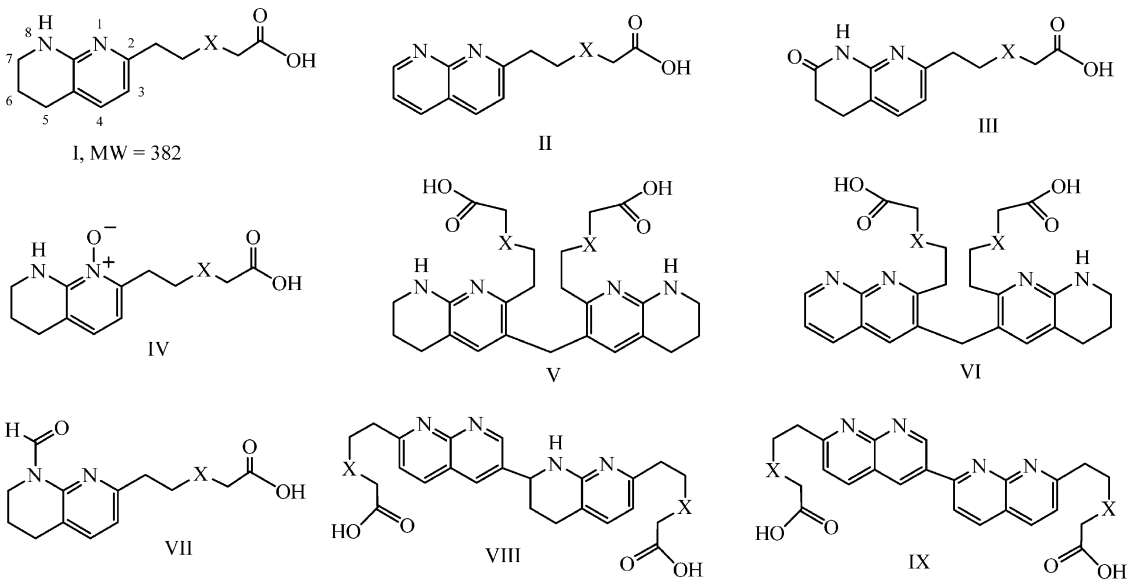

Fig. 1. Chemical structures of compound I and its major thermal degradates.

USA). Reagent-grade trifluoroacetic acid (TFA), phosphoric acid, and formaldehyde were from Aldrich Chemical Co. (Milwaukee, WI, USA). Deuterated water was from Isotec (Miamisburg, OH, USA).

2.2. Description of tablet formulations

The studied formulations were a mannitol-based tablet or an Avicel-based tablet, each containing 5 mg API. The major excipient, crystalline mannitol (Roquette, France) or Avicel PH101 (FMC Biopolymer, Newark, DE, USA), were used as diluents. Control tablets were made for each formulation by replacing the API with the respective diluent. All tablets were made by a high shear wet granulation process followed by drying, lubrication with magnesium stearate (Mallinckrodt Hazelwood, MO) and compression on a single station F-press (Manesty, Merseyside, UK).

2.3. Sample preparation and degradate isolation

The mannitol-based and Avicel-based tablets were stressed at 80 °C or 40 °C/75% RH stress conditions for 6 weeks. Control tablets for each formulation were stored at 5 °C for 6 weeks and were used for comparison. Each tablet containing 5 mg of compound I was stirred in 2.5 ml of 25/75 methanol–water (v/v) at 750 rpm for 1.5 h at ambient temperature in a 20 ml glass scintillation vial. The resulting mixtures were then transferred to 10 ml glass conical centrifuge tubes and centrifuged for 10 min at 3000 rpm at 10 °C. The supernatants were filtered with 0.45 μm nylon syringe filters. The filtered solutions were used for LC/MS analysis.

2.3.1. Generation and isolation of compound V

To generate compound V in quantities sufficient for nuclear magnetic resonance (NMR) analysis, 900 mg of the TRIS salt of compound I was dissolved in 30 ml of water. This solution was stressed at 80 °C for 1 month and used for HPLC separation without further treatment. Compound V, the major degradate under these conditions, was then isolated using semi-preparative HPLC. The HPLC method was developed using a Kromasil C_{18} (250 × 4.6 mm, 5 μm, 100 Å) analytical column from ThermoHypersil-Keystone (Bellefonte, PA, USA), and was then transferred to a semi-preparative Kromasil C_{18} (250 × 10 mm, 5 μm, 100 Å) column from ThermoHypersil-Keystone. The LC columns were eluted with 0.1% aqueous H_3PO_4 (A) and acetonitrile (B) at ambient temperature using the following binary gradient program: t = 0 min, 17%B; t = 20 min, 30%B; 25 min, 45%B; t = 26 min, 17%B. The flow rate was maintained at 1 ml min^{-1} during method development on the analytical column, and was kept at 4 ml min^{-1} for semi-preparative isolations. The collected fractions of compound V were combined, lyophilized, and submitted for NMR analysis.

2.3.2. Isolation of compounds VIII and IX

Degradates VIII and IX were isolated from a stressed Avicel formulation which was virtually identical to the mannitol formulation described above by replacing the mannitol with Avicel. The Avicel formulation stored at 50 °C/75% RH for 6 weeks was used since it produced a larger percentage of the degradates of interest than the mannitol formulation. The degradation profile in the Avicel formulation was similar to that of the mannitol formulation stored at 40 °C/75% RH. Approximately 20 stressed Avicel tablets containing 5 mg of compound I were stirred in 10 ml of 25/75 methanol–water (v/v) at 600 rpm for 1.5 h at ambient temperature. The resulting mixture was then filtered with 0.45 μm nylon syringe filters and used for HPLC separation. Again, the HPLC method was developed using a Kromasil C_{18} (250 × 4.6 mm, 5 μm, 100 Å) analytical column, and was then transferred to a semi-preparative Kromasil C_{18} (250 × 10 mm, 5 μm, 100 Å) column. The LC columns were eluted with 0.1% aqueous H_3PO_4 (A) and acetonitrile (B) at ambient temperature using the following binary gradient program: t = 0 min, 13%B; t = 40 min, 42%B; t = 41 min, 13%B. The flow rate was maintained at 1 ml min^{-1} during method development on the analytical column, and was kept at 4 ml min^{-1} for semi-preparative isolations. The collected fractions of compounds VIII and IX were combined,

respectively, lyophilized, and submitted for NMR analysis.

2.4. LC/MS and LC/UV instrumentation for degradate profiling

The HPLC system consisted of Shimadzu LC-10AD pumps with an SCL-10A system controller (Columbia, MD, USA). For on-line LC/MS and LC/MS/MS analyses of the stressed formulation samples and synthetic standards, a Waters Symmetry C18 column (4.6 × 250 mm, 5 μm, Milford, MA, USA) was eluted with 0.1% aqueous TFA (A) and acetonitrile (B) at ambient temperature using the following binary gradient program: t = 0 min, 10%B; t = 20–30 min, 20%B; 50 min, 46%B; t = 55–60 min, 80%B; t = 61 min, 10%B. The flow rate was maintained at 1 ml min^{-1} on the column, splitting at 15:85 ratio for LC/MS and LC/UV analyses. A PE series 200 autosampler (Perkin Elmer, Norwalk, CT, USA) was used for the sample injection. A solution of 50:50 acetonitrile/aqueous 0.1%TFA was used as the needle-wash solvent. An Agilent Model 1100 diode-array detector (Palo Alto, CA, USA) was used simultaneously for the analysis. The LC/UV trace at 244 nm was collected by the software which controlled the mass spectrometer.

For full-scan LC/MS and LC/MS/MS analyses, an Applied Biosystems API-300 triple quadrupole mass spectrometer (Applied Biosystems, Foster City, CA, USA) was operated in the positive ion mode with a TurboIonSpray™ interface. The ionization source temperature was 450 °C for all samples unless specified. An orifice voltage of 20 V was used for all experiments unless specified. In the full-scan experiments, the step size was 0.2 Da and the scan rate was 1 scan s^{-1} with variable scan ranges based on the objectives of the experiments. For the acquisition of LC/quasi-MS/MS/MS spectra, an orifice voltage of 80 V was used to initiate the in-source fragmentation. In quasi-MS/MS/MS experiments, fragment ions of the target molecule are first generated in the ionization source region at high orifice voltages. The specific fragment ions of interest are then selected by the first quadrupole (Q1) followed by fragmentation in the collision cell (Q2) with nitrogen gas, and finally full-scan detection of the second-generation fragment ions is made by the third quadrupole (Q3).

2.5. NMR instrumentation

All spectra were acquired on a Varian Unity Inova 600 MHz NMR spectrometer (Varian, Palo Alto, CA) equipped with a 5 mm Nalorac $^{1}H\{^{13}C/^{15}N\}$ PFG triple resonance probe (Nalorac, Martinez, CA, USA). 1H-1D, TOCSY, NOE and 2D spectra of COSY, HSQC, and HMBC were obtained at 25 °C for the structural analysis of degradates V, VIII, and IX with purified material dissolved in D_2O. Similar experiments were also performed for compound I in D_2O for comparison.

3. Results and discussion

The stressed and control formulations were analyzed by LC/MS with simultaneous diode array detection. Fig. 2 shows the LC/MS total ion chromatogram (TIC, top panel) and LC/UV chromatogram at 244 nm (bottom panel) for the mannitol/wet granulation formulation stressed at 80 °C for 6 weeks. In comparison, Fig. 3 shows the LC/MS TIC (top panel) and LC/UV chromatogram at 244 nm (bottom panel) for the same formulation stored at 5 °C for 6 weeks. By combining the LC/UV and LC/MS data, eight major and three minor degradates were detected in the stressed sample. Among the eight major degradates, two of them co-eluted at a retention time (RT) of 38.2 min and another two dimeric degradates co-eluted at RT of 40.4 min. LC/MS/MS data of the parent drug and major degradates suggested that the primary structural changes occurred to the tetrahydronaphthyridine portion of the molecule. Therefore, a good understanding of the gas phase fragmentation of the protonated compound I would be essential for the structural elucidation of the unknowns.

3.1. Fragmentation of protonated compound I

The product ion spectrum of the protonated compound I (m/z 383) is displayed in the top panel

of Fig. 4. For compound I, protonation of either the carboxylic group (pathway 1) or the naphthyridine ring (pathway 2) can lead to the formation of fragment ions (Scheme 1). Apparently, the loss of a water molecule from the protonation of the carboxylic group followed by the loss of a ketene

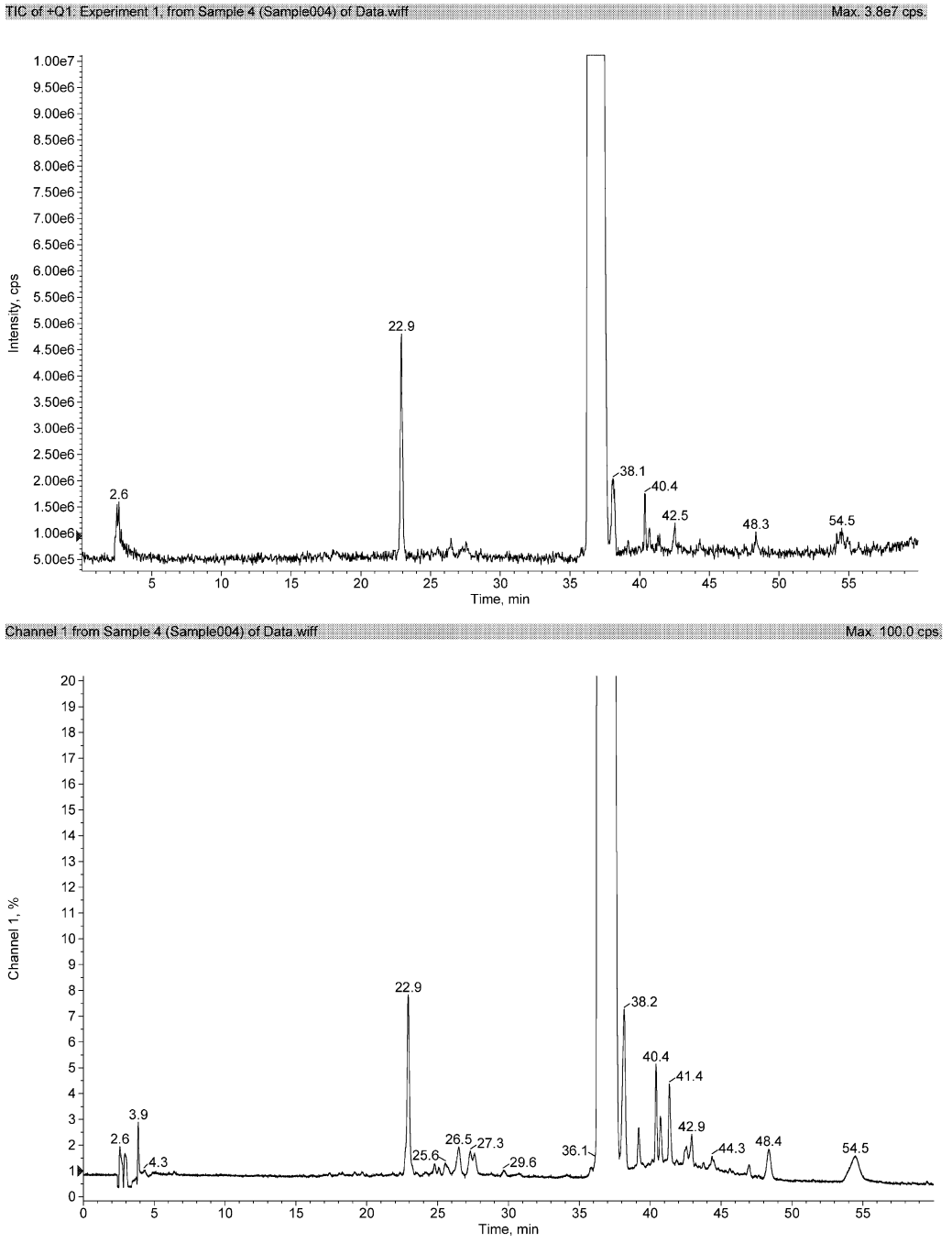

Fig. 2. LC/MS TIC (top panel) and LC/UV chromatogram at 244 nm (bottom panel) for the stressed mannitol/wet granulation formulation (80 °C/6 weeks).

produced fragment ions at m/z 365 and 323, respectively. The ions at m/z 175, 161, and 147 appeared to be generated by the fragment ion at m/z 323. This postulation was supported by the experimental data in which quasi-MS^3 of the ion at m/z 323 (i.e. generation of the fragment ion at m/z

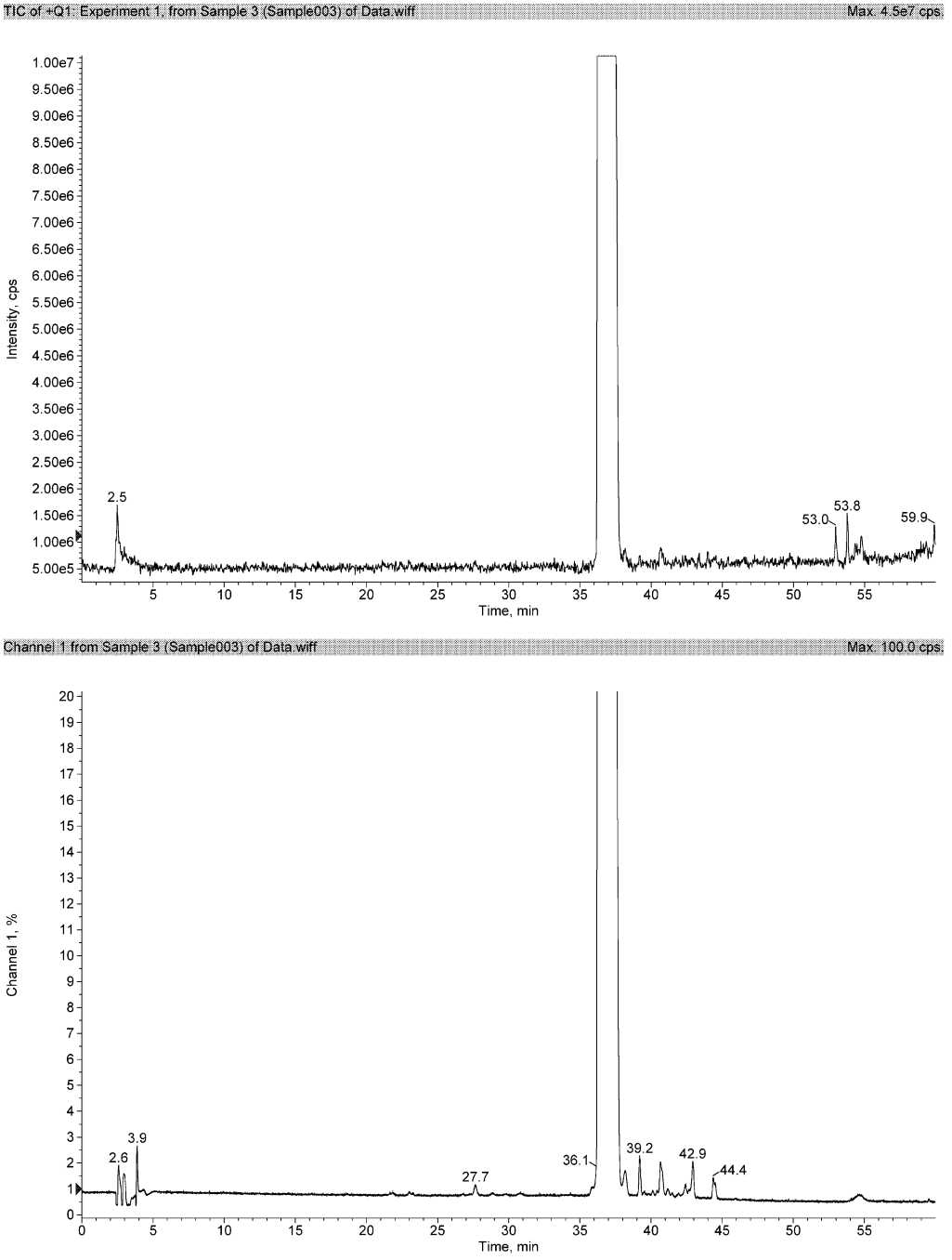

Fig. 3. LC/MS TIC (top panel) and LC/UV chromatogram at 244 nm (bottom panel) for the control mannitol/wet granulation formulation (5 °C/6 weeks).

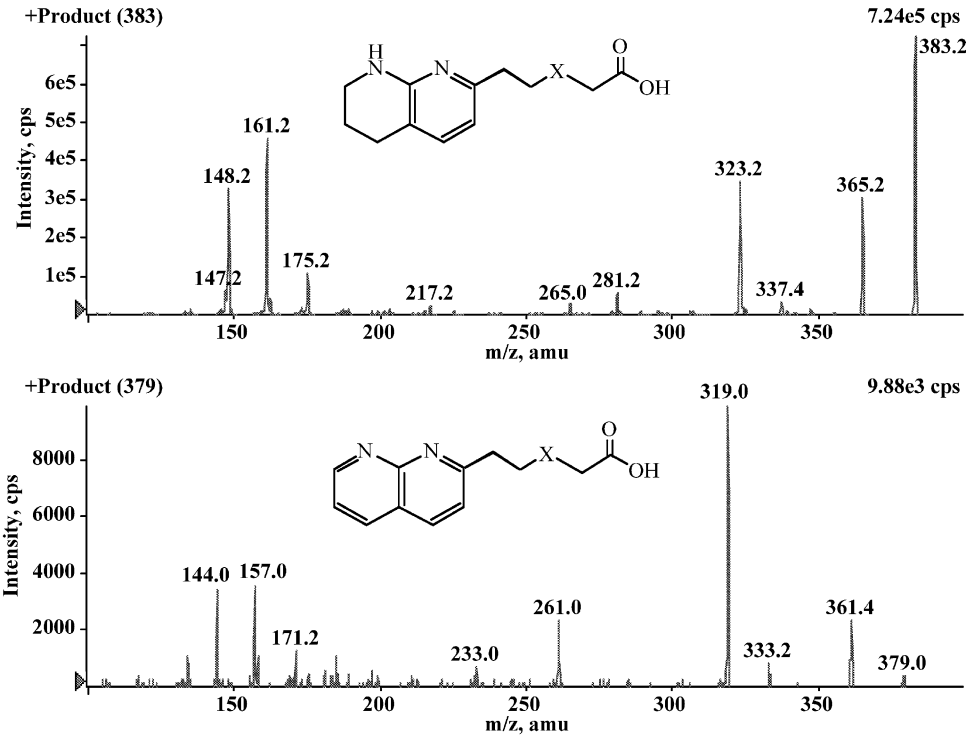

Fig. 4. Product ion spectra of protonated compound I (top panel) and protonated degradate II (bottom panel). Collision energy of 43 eV for both compounds.

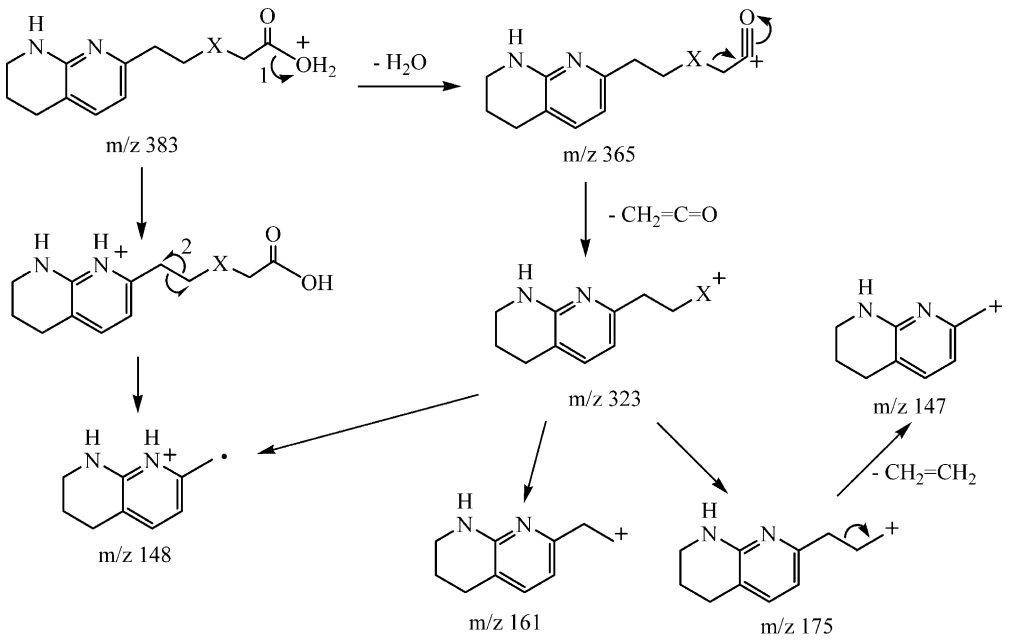

Scheme 1. Proposed fragmentation pathways for protonated compound I.

323 through in-source collision-induced dissociation (CID) followed by MS/MS in the Q2 indeed yielded the above ions plus an ion at m/z 148. The alternative pathway for the formation of the ion at m/z 148 is through a homolytic cleavage of the C–C bond from the protonated naphthyridine. These data indicated that the naphthyridine moiety was preserved during the fragmentation process. This observation was essential for the structural proposal for several major degradates including the M-4 (M stands for compound I), the amide, and the N-oxide (compounds II–IV in Fig. 1).

3.2. Degradates II–IV

The product ion spectrum (Fig. 4, bottom panel) of the primary degradate at RT = 22.9 was acquired under the same LC/MS/MS conditions as those for compound I. A shift of 4 Da for all fragment ions clearly indicated that the loss of four hydrogen atoms occurred on the tetrahydronaphthyridine. This result was not surprising since oxidation of the tetrahydronaphthyridine leads to the formation of a fully aromatized product, compound II. This structural proposal was further confirmed by the observation of such kind of aromatized product from the degradation of a close structural analog of compound I, where an authentic standard of the aromatized degradate was synthesized.

Despite shifts of m/z values of 14 and 16 units, degradates III and IV (co-eluted at RT = 38.2 min) also displayed very similar fragment ion profiles (data not shown) to that of the compound I, suggesting the additions of 14 and 16 Da occurred on the tetrahydronaphthyridine moiety. With the availability of synthetic standards for both compounds, their identities were confirmed by RT and MS/MS spectra. The possible formation mechanism for these three major degradates will be discussed in Section 3.4.

3.3. API–TRIS interactions—formation of methylene-bridged dimers

It was observed that higher molecular weight degradates (MW = 776 and 772) at RT = 40.4 min and the M+28 degradate at RT = 48.4 min were also among the major degradates when the formulations were stressed at 80 °C. These degradates were negligible when the samples were stored at 40 °C/75% RH for 6 weeks. Based on the molecular weight difference, it was assumed that the degradate with MW of 772 was the aromatized form of the degradate with MW of 776, similar to the structural change from I to II. The product ion spectrum (Fig. 5, bottom panel) of the doubly charged ion at m/z 389 for the degradate with MW of 776 generated abundant fragment ions at m/z 395 and 383. Quasi-MS^3 experiments were performed for both ions at m/z 395 and 383. The latter ion showed an identical MS/MS profile as that of compound I, while the quasi-MS^3 spectrum of the former ion suggested an addition of 14 Da to the naphthyridine portion. These data indicated a possible dimeric structure linked by a single unit such as $-CH_2-$ or $-O-$ for the unknown, depending on the degree of aromatization of the two tetrahydronaphthyridines. The fact that these degradates only formed at high temperature seemed to be consistent with the literature report on the thermal degradation of TRIS [5]. This postulation was confirmed with the generation of the same dimeric degradate by stressing a mixture of compound I (free drug, zwitter ion form) and formaldehyde in water at 80 °C for 3 weeks. The desired degradate was later isolated by semi-preparative HPLC from a stressed TRIS salt solution of compound I in water at 80 °C for 1 month.

The isolated degradate was subjected for LC/MS and ^1H- and ^{13}C-NMR analyses. Table 1 summarizes the hydrogen and carbon chemical shifts for the aromatic regions and the bridging carbon atom. The 1D proton spectrum of compound V showed one singlet in the aromatic region that integrated to two protons. 2D COSY data indicated protons BH5, BH6 and BH7 are in one spin system, and each of the peaks integrated to four protons in the 1D spectrum. 1D NOE data showed that proton AH4 is close to protons H11 and BH5, and proton H11 is close to proton AH4, and other protons on the chain. Key correlations observed in the HMBC experiment were the three-bond correlation of proton AH4 to carbons C11, BC5, AC2 and AC9, the two-bond correlation of

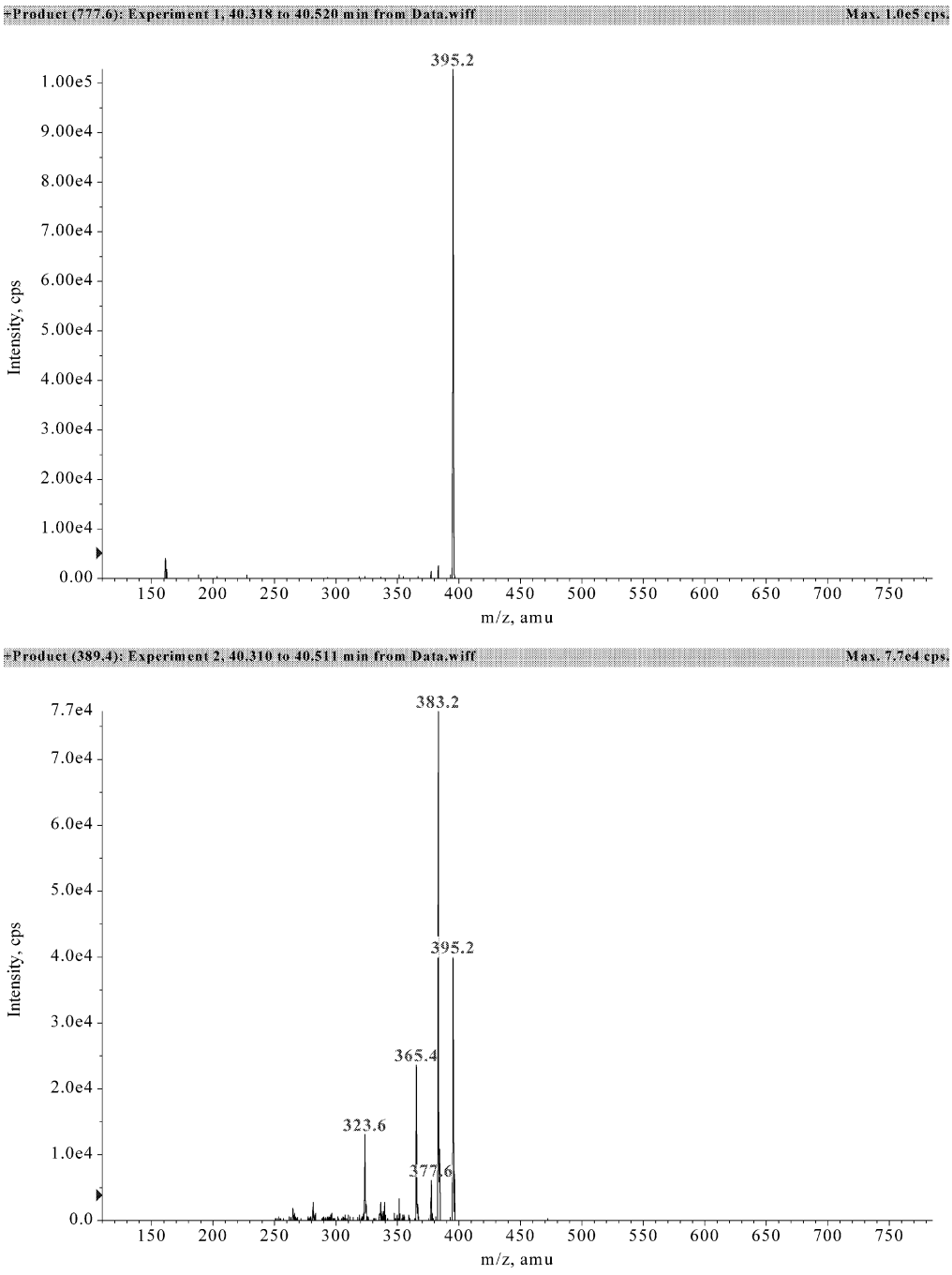

Fig. 5. Product ion spectra of the singly charged (top panel) and doubly charged (bottom panel) ions of degradate V. Collision energy of 55 and 40 eV for the singly and doubly charged ions, respectively.

Table 1
Chemical shift (aromatic region) assignments for the dimeric degradate V

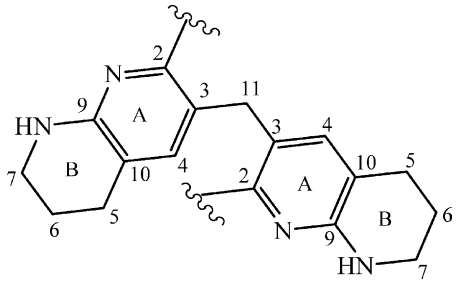

Assignment		Carbon, $^{\delta}$C (ppm)	Proton, $^{\delta}$H (ppm)
11	CH_2	32.87	3.772 (s)
A			
2	2 × C	148.44	
3	2 × C	122.77	
4	2 × CH	145.75	7.319 (s)
9	2 × C	152.88	
10	2 × C	122.41	
B			
5	2 × CH_2	27.58	2.719 (t, J = 6.0 Hz)
6	2 × CH_2	21.74	1.891 (m)
7	2 × CH_2	43.58	3.451 (t, J = 5.2 Hz)

proton H11 to carbon AC3, and the three-bond correlation of proton H11 to carbons AC2 and AC4. These data clearly showed the presence of a methylene group linked dimer V.

The formation of fragment ions at m/z 395 and 383 from the doubly charged ion of degradate V also supported this structural assignment (Scheme 2). It should be noted that the fragmentation of the singly charged degradate V produced almost exclusively the fragment ion at m/z 395 (Fig. 5, top panel). This result was not surprising since the resulting fragment ion was favored by resonance stabilization. Although the co-eluting degradate with MW of 772 was not isolated for extensive characterization, its LC/MS/MS data undoubtedly indicated the formation of fragment ions at m/z 391 and 383 (data not shown), implying a close structural analog of degradate V. The fragmentation mechanism shown in Scheme 2 for degradate V can also easily explain why the carbocation resides on the fully aromatized naphthyridine (i.e. m/z 391), not on the tetrahydronaphthyridine. The formation of these two unique degradates (Scheme 3) can be rationalized by in situ generated formaldehyde reacting with compound I to form a hydroxymethyl intermediate [6]. This intermediate could lose a water molecule to generate a more reactive methide intermediate which further reacts with compound I to give rise to degradate V. Oxidation of degradate V would lead to the formation of degradate VI.

The M+28 degradate was not isolated for NMR analysis, however, the product ion spectrum of protonated VII clearly indicated the loss of a CO in the gas phase to re-generate the protonated compound I. Again, the source of this single carbon is believed to be the TRIS. Scheme 4 presents a proposed mechanism for the formation of an N-formyl degradate. Similar to the reaction shown in Scheme 3, a different intermediate, N-hydroxymethyl derivative, formed initially followed by oxidation to generate a more stable N-formyl product.

A minor degradate (MW = 485) derived from condensation of compound I and TRIS was also detected at RT = 26.5 min. The MS/MS data were insufficient to confirm whether the degradate is an amide or an ester since both the amino group and three hydroxyl groups of the TRIS can potentially react with compound I.

3.4. Dimeric degradates directly derived from compound I

The remaining two high molecular weight degradates (MW = 758 and 754) were detected (RT = 40.4 and 41.4 min) under both stress conditions. Their formation appeared to be facilitated by increased moisture level. Fig. 6 presents the product ion spectra of the singly and doubly charged degradate with MW of 758. These spectra were quite complicated and not straightforward for the deduction of the unknown structures.

Isolation of both degradates by semi-preparative HPLC from the stressed formulations was followed by ^{1}H- and ^{13}-NMR analyses. Table 2 summarizes the hydrogen and carbon chemical

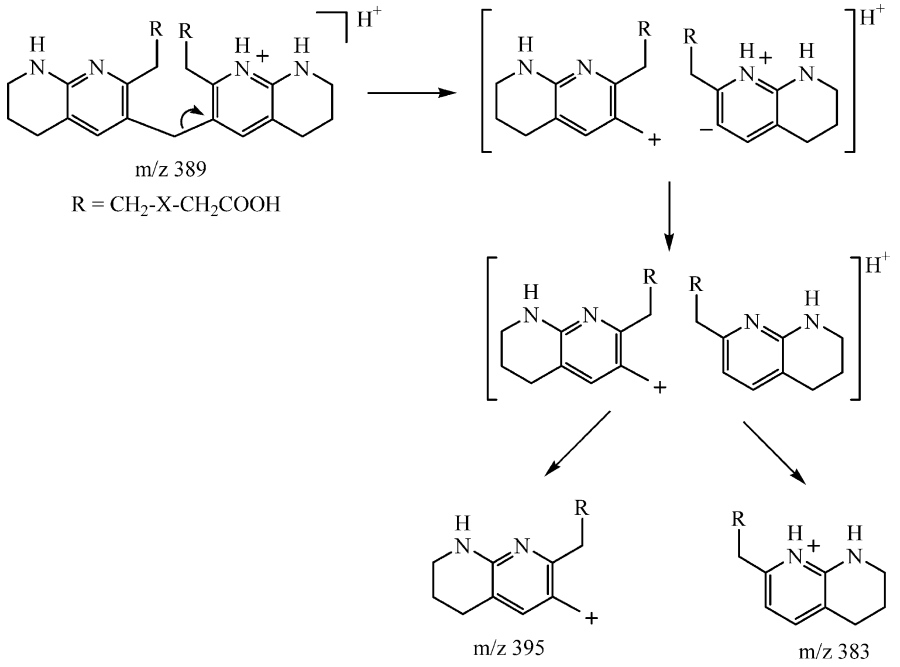

Scheme 2. Tentative fragmentation mechanism for the doubly charged degradate V.

shifts of the aromatic regions for degradate VIII. The 1D proton spectrum of compound VIII indicated that, for rings A, B and D, four aromatic protons had $J_{ortho} = 8.6$ Hz, and two aromatic protons had $J_{meta} = 1.8$ Hz. The chemical shift assignment in Table 2 was partly obtained from the analysis of 1D TOCSY and 2D COSY to establish spin systems, and 1D NOE from targets at various aromatic ring protons to determine their spatial proximity. Crucial correlations observed in the HMBC experiment were the two-bond correlation of proton CH7′ to carbons BC6 and BC6′, and the three-bond correlation of proton CH7′ to carbons BC5 and BC7. These data proved the formation of C–C bond between BC6 and CC7′ carbons for the dimer.

The unique linkage of this dimer can be rationalized by an initial N-α-hydroxylation of the tetrahydronaphthyridine followed by dehydration to form an imine and an enamine (Scheme 5). The subsequent addition of the enamine to the imine followed by oxidation can lead to the formation of VIII. Further oxidation of VIII would result in the formation of the aromatized dimer IX which was also confirmed by NMR spectroscopy (data not shown). This proposed mechanism is supported by the observation that both 7- and 5-monohydroxylated and 5,7-bishydroxylated products became noticeable under high humidity conditions (data not shown). In fact, the presence of the 7-hydroxylated product (X in Scheme 5) of compound I in all stressed formulation samples was confirmed by a synthetic standard based on RT and MS/MS profile. The degradation pathways illustrated in Scheme 5 also include the formation mechanism for other major degradates such as II–IV.

The fragmentation patterns of the two dimeric degradates (VIII and IX) provided strong support for the structural assignments from NMR. Scheme 6 shows that the singly charged VIII produces unique fragment ions at m/z 405 and 355 via a retro-Diels-Alder reaction [7,8]. Similar to the fragmentation of compound I, the doubly charged VIII (m/z 380) would yield doubly charged fragment ions at m/z 350 and 320 (Scheme 7).

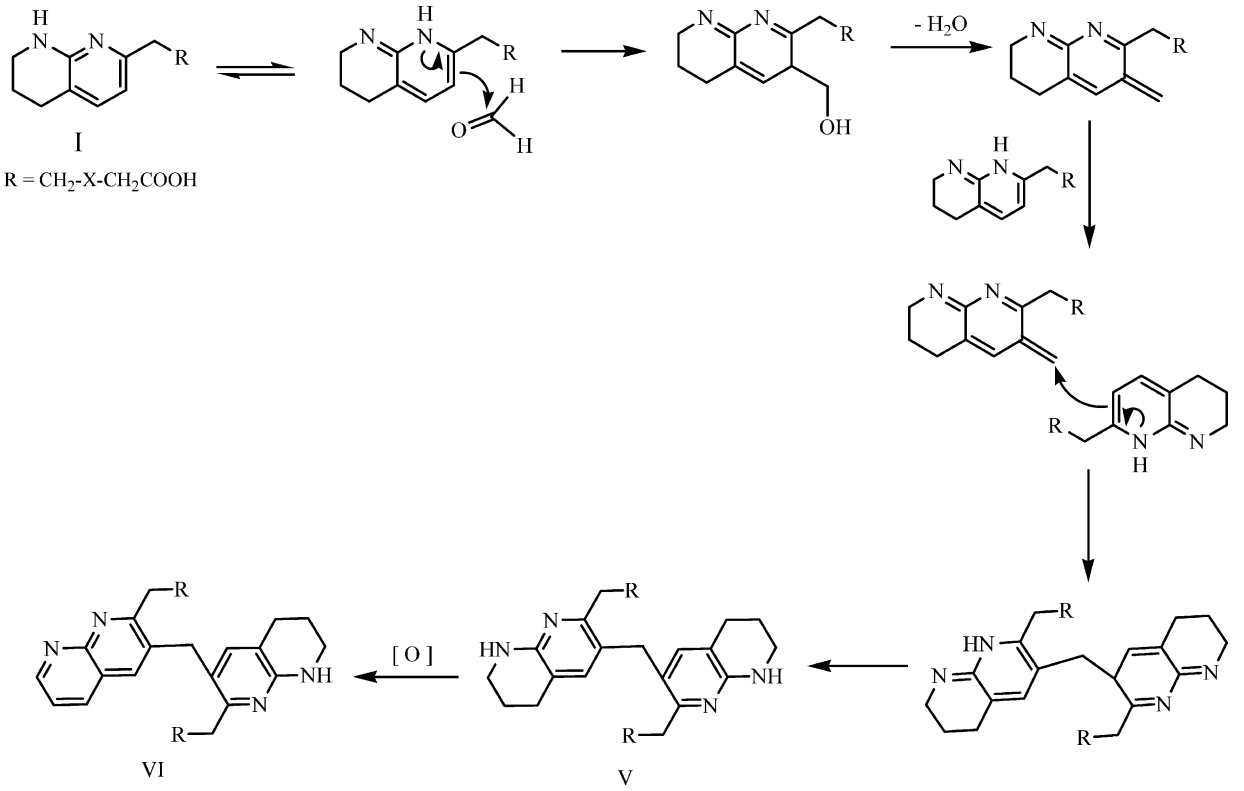

Scheme 3. Possible formation mechanism for degradates V and VI.

3.5. Drug–excipient interactions

It has been well-documented in the literature that the chemical interactions between the drug and formulation excipients can lead to the formation of undesirable degradates [9–11]. Examples of drugs containing carboxylic groups reacting with excipients have also been previously reported [12]. In this study, two isomeric condensation products (MW = 546) between compound I and mannitol

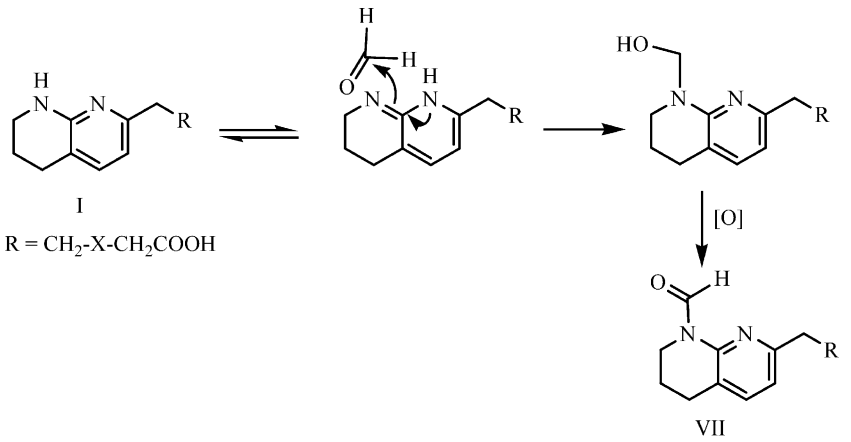

Scheme 4. Possible formation mechanism for degradate VII.

were detected in the thermal stressed samples (RT = 27.3 and 27.6 min). Although the MS/MS data were not sufficient to pinpoint the linkage, the drug–excipient interactions at elevated temperature was certain. These condensation products were negligible when the formulations were

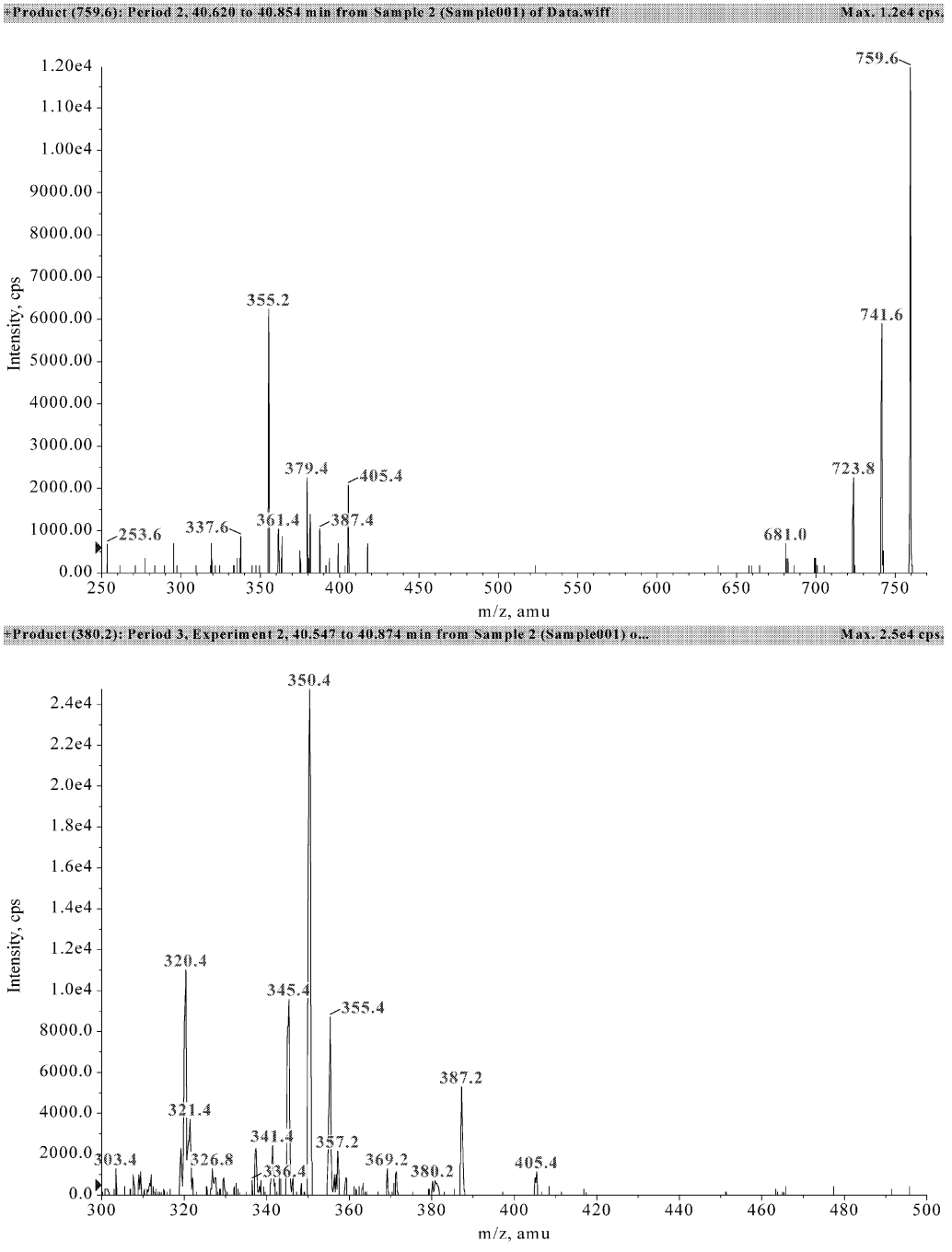

Fig. 6. Product ion spectra of the singly charged (top panel) and doubly charged (bottom panel) ions of degradate VIII. Collision energy of 55 and 40 eV for the singly and doubly charged ions, respectively.

stressed under 40 °C/75% RH conditions. These results are expected since higher temperature promotes the loss of water which is the by-product of condensation reactions.

4. Conclusions

Among the various causes of drug degradation, oxidation has been one of the most commonly seen degradation pathways for many formulations [13,14]. This is especially true for compound I which underwent N-oxidation and N-α-hydroxylation (i.e. C-oxidation). The unstable 7-hydroxylated degradate further yielded the aromatized product, the amide, and the dimers. The high abundance of dimeric degradates may be related to the close proximity (4.8 Å) of the two tetrahydronaphthyridine rings in the solid state as evidenced by the single crystal structure of compound I [15]. The fact that higher humidity conditions facilitate the formation of degradates VIII and IX reflects possible formation of local amorphous structures which are advantageous for inter-molecular reactions.

Although the interaction between the API and its counterion has been previously reported [16], the thermal degradation of TRIS deserves additional comments since the in situ generated formaldehyde can react with a variety of functional groups. Many impurities and degradates derived from formaldehyde have been identified in pharmaceutical formulations [17–23]. The source of formaldehyde varied from degradation of the API or excipients, impurities present in the excipients, to leakage from packaging materials. Even though the TRIS salt of compound I has superior aqueous solubility and mechanical properties, its chemical stability under various stress conditions needs to be considered during the final salt selection process. The data generated herein as well as the published results indicated that TRIS becomes unstable at a temperature of over 70 °C. Despite the absence of formaldehyde-derived degradates in the samples stressed at 40 °C/75% RH for 6 weeks, long term stability of the TRIS salt at a temperature lower than 70 °C should be carefully monitored to ensure the viability of the formulation. Based on the results of this study, precaution should be taken during the salt selection process, especially for the organic salts. The potential interactions between the API and its counterion and/or degradates from the counterion should be evaluated at an early stage to avoid significant loss of time and waste of resources.

The current study again illustrated that excipients are better known as promoters of degradation than as stabilizers of drug substances. The condensation products produced from the reactions of compound I with mannitol and TRIS are typical examples of drug–excipient interactions in formu-

Table 2
Chemical shift (aromatic region) assignments for the dimeric degradate VIII

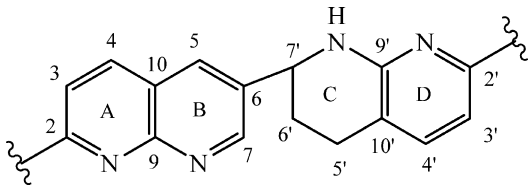

Assignment		Carbon, $^{\delta}$C (ppm)	Proton, $^{\delta}$H (ppm)
A			
2	C	168.69	
3	CH	127.26	8.019 (d, J = 8.6 Hz)
4	CH	149.37	8.957 (d, J = 8.6 Hz)
9	C	148.86	
10	C	125.27	
B			
5	CH	139.84	8.682 (d, J = 1.8 Hz)
6	C	141.85	
7	CH	157.46	9.200 (d, J = 1.8 Hz)
C			
5′	H–C–H′	24.70	2.898, 2.669 (m)
6′	H–C–H′	29.69	2.350, 2.212 (m)
7′	CH	55.10	5.273 (t, J = 5.3 Hz)
D			
2′	C	152.20	
3′	CH	114.91	6.766 (d, J = 8.6 Hz)
4′	CH	145.46	7.708 (d, J = 8.6 Hz)
9′	C	153.25	
10′	C	121.38	

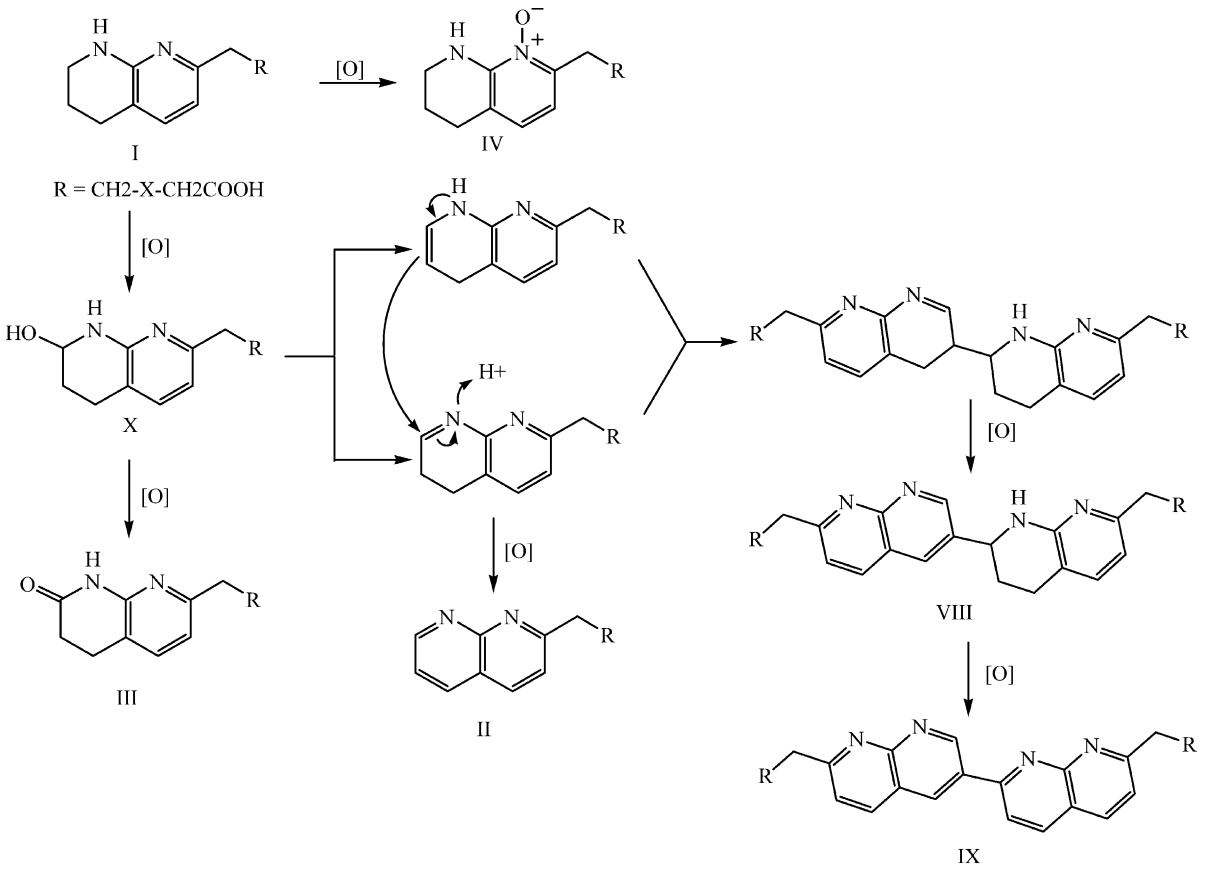

Scheme 5. Possible formation mechanism for degradates II–IV and VIII–X.

lations. Therefore, selection of formulation excipients during drug development process should also consider the potential interactions between the drug molecules and the inactive ingredients (e.g. Mallard reaction of lactose and primary/secondary amines [24,25]).

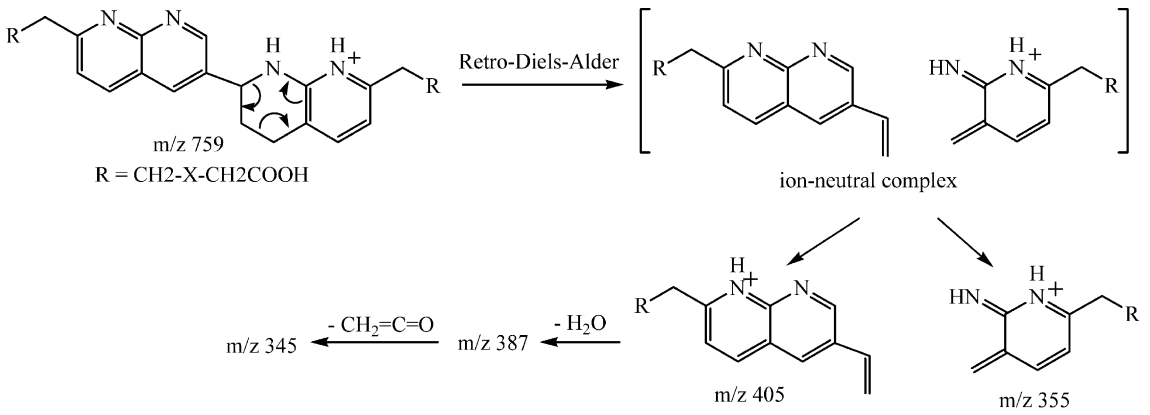

Scheme 6. Proposed fragmentation mechanism for protonated degradate VIII.

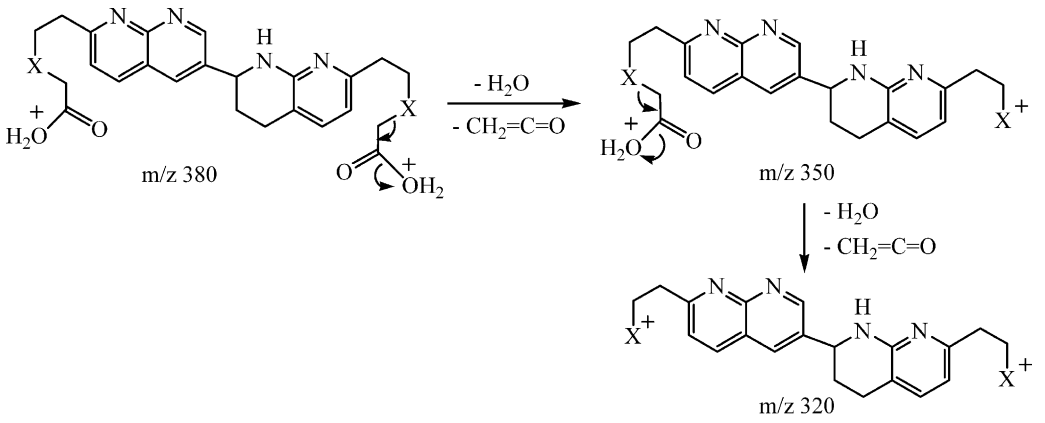

Scheme 7. Proposed fragmentation mechanism for the doubly charged degradate VIII.

The current study also demonstrated that the combination of LC/MS/MS and NMR techniques is essential for solving such complicated problems. LC/MS/MS alone may not be sufficient to pinpoint the locations of structural modifications since fragment information is often limited due to either the difficulty in breaking the specific portion of the molecules in the gas phase or the difficulty in interpreting the fragmentation patterns.

Acknowledgements

The authors would like to thank Dr Paul Coleman for providing the synthetic standards of degradates II–IV and X. We would also like to thank Professor Joseph P. Dinnocenzo of University of Rochester for his valuable discussion on the formation mechanism of degradate VIII. Finally, we would like to express our sincere thanks to Dr Robert Reed for his critical review of the manuscript.

References

[1] R.J. Bastin, M.J. Bowker, B.J. Slater, Org. Proc. Res. Dev. 4 (2000) 427–435.
[2] M.L. Cotton, P. Lamarche, S. Motola, E.B. Vadas, Int. J. Pharm. 109 (1994) 237–249.
[3] K.R. Morris, M.G. Fakes, A.B. Thakur, A.W. Newman, A.K. Singh, J.J. Venit, C.J. Spagnuolo, A.T.M. Serajuddin, Int. J. Pharm. 105 (1994) 209–217.
[4] Y. Wu, H. Wang, W. Xu, K. Algayer, T.-L. Hwang, A. Procopio, L. DeBusi, C. Yang, B. Matuszewska, presented the preliminary results at the 50th ASMS Conference on Mass Spectrometry and Allied Topics, Orlando, FL, 2002.
[5] Y. Song, R.L. Schowen, R.T. Borchardt, E.M. Topp, J. Pharm. Sci. 90 (2001) 1198–1203.
[6] D.E. Minter, M.A. Re, J. Org. Chem. 53 (1988) 2653–2655.
[7] N. Martin, R. Martinez-Alvarez, C. Seoane, M. Suarez, E. Salfran, Y. Verdecia, N.K. Sayadi, Rapid Commun. Mass Spectrom. 15 (2001) 20–24.
[8] G. Dannhardt, I. Obergrusberger, J. Kiermaier, K.K. Mayer, Arch. Pharm. 319 (1986) 735–744.
[9] P.J. Crowley, Pharm. Sci. Technol. Today 2 (1999) 237–243.
[10] P.J. Crowley, L. Martini, Pharm. Tech. Europe 13 (2001) 26–34.
[11] S.R. Byrn, W. Xu, A.W. Newman, Adv. Drug Deliv. Rev. 48 (2001) 115–136.
[12] P. Kahela, L. Liponkoski, T. Huemerinta, Acta Pharm. Fenn. 88 (1979) 113–116.
[13] Y. Wu, Biomed. Chromatogr. 14 (2000) 384–396.
[14] M.S. Lee, E.H. Kerns, Mass Spectrom. Rev. 18 (1999) 187–279.
[15] Y.-H. Kiang, Merck internal memos.
[16] S.A. Schildcrout, D.S. Risley, R.L. Kleemann, Drug Dev. Ind. Pharm. 19 (1993) 1113–1130.
[17] E. Doelker, A.C. Vial-Bernasconi, STP Pharm. 4 (1988) 298–306.
[18] D.S. Bindra, T.D. Williams, V.J. Stella, Pharm. Res. 11 (1994) 1060–1064.

[19] D.S. Desai, B.A. Rubitski, J.S. Bergum, S.A. Varia, Int. J. Pharm. 110 (1994) 257–265.
[20] D.S. Desai, B.A. Rubitski, S.A. Varia, M.H. Huang, Int. J. Pharm. 107 (1994) 141–147.
[21] E.J. Delaney, R.G. Sherrill, V. Palaniswamy, T.C. Sedergran, S.P. Taylor, Steroids 59 (1994) 196–204.
[22] S. Rubnov, I. Shats, D. Levy, S. Amisar, H. Schneider, J. Pharm. Pharmacol. 51 (1999) 9–14.
[23] X.-Z. Qin, D.P. Ip, K.H.-C. Chang, P.M. Dradransky, M.A. Brooks, T. Sakuma, J. Pharm. Biomed. Anal. 12 (1994) 221–233.
[24] D.D. Wirth, S.W. Baertschi, R.A. Johnson, S.R. Maple, M.S. Miller, D.K. Hallenbeck, S.M. Gregg, J. Pharm. Sci. 87 (1998) 31–39.
[25] R.C. George, R.J. Barbuch, E.W. Huber, B.T. Regg, Drug Dev. Ind. Pharm. 20 (1994) 3023–3032.